



# Deubiquitinase OTUD5 is a positive regulator of mTORC1 and mTORC2 signaling pathways

Jin Hwa Cho<sup>1</sup> · Kidae Kim<sup>1,2</sup> · Sung Ah Kim<sup>1,3</sup> · Sungryul Park<sup>1,3</sup> · Bi-Oh Park<sup>1,4</sup> · Jong-Hwan Kim<sup>5</sup> · Seon-Young Kim<sup>3,5</sup> · Min Jee Kwon<sup>6</sup> · Myeong Hoon Han<sup>6</sup> · Sung Bae Lee<sup>6</sup> · Byoung Chul Park<sup>1,2</sup> · Sung Goo Park<sup>1,3</sup> · Jeong-Hoon Kim<sup>1,3</sup> · Sunhong Kim<sup>1,7,8</sup>

Received: 15 January 2020 / Revised: 12 October 2020 / Accepted: 14 October 2020 / Published online: 27 October 2020  
© The Author(s), under exclusive licence to ADMC Associazione Differenziamento e Morte Cellulare 2020

## Abstract

The mammalian Target of Rapamycin (mTOR) pathway regulates a variety of physiological processes, including cell growth and cancer progression. The regulatory mechanisms of these signals are extremely complex and comprise many feedback loops. Here, we identified the deubiquitinating enzyme ovarian tumor domain-containing protein 5 (OTUD5) as a novel positive regulator of the mTOR complex (mTORC) 1 and 2 signaling pathways. We demonstrated that OTUD5 stabilized  $\beta$ -transducin repeat-containing protein 1 ( $\beta$ TrCP1) proteins via its deubiquitinase (DUB) activity, leading to the degradation of Disheveled, Egl-10, and pleckstrin domain-containing mTOR-interacting protein (DEPTOR), which is an inhibitory protein of mTORC1 and 2. We also showed that mTOR directly phosphorylated OTUD5 and activated its DUB activity. RNA sequencing analysis revealed that OTUD5 regulates the downstream gene expression of mTOR. Additionally, OTUD5 depletion elicited several mTOR-related phenotypes such as decreased cell size and increased autophagy in mammalian cells as well as the suppression of a *dRheb*-induced curled wing phenotype by RNA interference of *Duba*, a fly ortholog of *OTUD5*, in *Drosophila melanogaster*. Furthermore, OTUD5 knockdown inhibited the proliferation of the cancer cell lines with mutations activating mTOR pathway. Our results suggested a positive feedback loop between OTUD5 and mTOR signaling pathway.

---

Edited by D. Guardavaccaro

**Supplementary information** The online version of this article (<https://doi.org/10.1038/s41418-020-00649-z>) contains supplementary material, which is available to authorized users.

---

✉ Sung Goo Park  
sgpark@kribb.re.kr

✉ Jeong-Hoon Kim  
jhoonkim@kribb.re.kr

✉ Sunhong Kim  
skimworm@gmail.com

- <sup>1</sup> Disease Target Structure Research Center, KRIBB, Daejeon 34141, Republic of Korea
- <sup>2</sup> Department of Proteome Structural Biology, KRIBB School of Biological Science, Korea University of Science and Technology, Daejeon 34113, Republic of Korea
- <sup>3</sup> Department of Functional Genomics, KRIBB School of Biological

## Introduction

The mTOR signaling pathway plays a key role in sensing and integrating a variety of environmental cues and coordinating many cellular processes necessary for cell growth and proliferation [1]. mTOR functions through two distinct complexes: mTOR complex (mTORC) 1 and 2. In response

- Science, Korea University of Science and Technology, Daejeon 34113, Republic of Korea
- <sup>4</sup> College of Pharmacy, Chungbuk National University, Cheongju 34113, Republic of Korea
  - <sup>5</sup> Personalized Genomic Medicine Research Center, KRIBB, Daejeon 34141, Republic of Korea
  - <sup>6</sup> Department of Brain & Cognitive Sciences, DGIST, Daegu 42988, Republic of Korea
  - <sup>7</sup> Department of Biomolecular Science, KRIBB School of Biological Science, Korea University of Science and Technology, Daejeon 34113, Republic of Korea
  - <sup>8</sup> Present address: Drug Discovery Center, Life Sciences, LG Chem, Seoul 07796, Republic of Korea

to nutrients, energy, and growth factors, mTORC1 phosphorylates various substrates, such as p70 S6 kinase (S6K), eukaryotic translation initiation factor 4E-binding protein (4EBP), and UNC-51-like kinase (ULK1), which promotes the synthesis of macromolecules and regulates autophagy. mTORC2 is mainly activated by growth factors such as insulin [2, 3]. Once activated, mTORC2 phosphorylates the AGC kinase family, such as Akt, serum- and glucocorticoid-inducible kinase (SGK), and protein kinase C (PKC), and promotes cell survival, proliferation, and cytoskeletal organization [1–3].

Ubiquitination is one of the important cellular processes that regulates mTOR signaling [4]. Such protein ubiquitination can be reversed by a deubiquitinase (DUB). Recently, several studies have revealed that DUBs catalyze the removal of the ubiquitin moiety on mTOR signaling components [4]. For example, belonging to the ovarian tumor domain (OTU) family DUBs, OTUB1 plays a role in stabilizing the endogenous mTOR inhibitor DEPTOR [5], leading to the inhibition of mTORC1 signaling activity [5]. UCHL1 and OTUD7B are responsible for the cleavage of polyubiquitin chains of Raptor and G $\beta$ L, respectively [6, 7].

OTUD5 is a DUB belonging to the OTU family and was first identified as a negative regulator of type I interferon production by removing K63-linked ubiquitin chains of TNF receptor-associated factor 3 (TRAF3) [8]. In addition, OTUD5 suppresses T<sub>H</sub>17 differentiation by stabilizing UBR5 [9]. In this study, we identified OTUD5 as a novel positive regulator of both the mTORC1 and mTORC2 pathways. OTUD5 deubiquitinated and stabilized  $\beta$ TrCP1, leading to the downregulation of DEPTOR. Additionally, mTOR per se phosphorylated OTUD5, which appeared to be necessary for its DUB activity. Finally, we demonstrated that OTUD5 regulated various downstream of mTOR signaling, including cell size, proliferation, and autophagy. Collectively, our results suggested that OTUD5 and mTOR positively regulated each other.

## Materials and methods

### Antibodies and reagents

Anti-OTUD5 antibody (ab176727) was purchased from Abcam (Cambridge, UK). Primary antibodies against S6K (2708), S6K(p)Thr389 (9234), 4EBP1 (9644), 4EBP1(p)Thr37/46 (2855), Akt (4691), Akt(p)Ser473 (4060), DEPTOR (11816),  $\beta$ TrCP1 (4394), mTOR (2983), TSC1 (6935), TSC2 (3990), G $\beta$ L (3274), UBR5 (65344), AMPK (2532), AMPK(p)Thr172 (2531), LC3A/B (12741) and Myc-tag (2278) were obtained from Cell Signaling Technology (Danvers, MA, USA). Anti-p62 antibody (M162-3) was purchased from MBL (Woburn, MA, USA). Anti-

Flag<sup>®</sup> M2 (F3165 and F7425), M2 magnetic beads (M8823), and anti-tubulin (T5168) antibodies were purchased from Sigma Aldrich (St. Louis, MO, USA). Anti-HA antibody (11867423001) was purchased from Roche (Basel, Switzerland). Anti-Myc (sc-40) and anti-GAPDH (sc-47724) antibodies were obtained from Santa Cruz Biotechnology (Dallas, TX, USA). Anti-Armadillo antibody was purchased from Developmental Studies Hybridoma Bank (Iowa, IA, USA). Polyclonal anti-OTUD5(p)S503 antibody was generated in a rabbit using a synthetic phosphopeptide derived from 500–512 amino acids of human OTUD5 as the immunogen by AbClon (Seoul, Republic of Korea). Anti-HA magnetic beads (88837), anti-c-Myc magnetic beads (88843), and anti-DYKDDDDK magnetic beads (A36798) were obtained from Thermo Fisher Scientific (Waltham, MA, USA). Rapamycin (R8781), MG132 (C2211), blasticidine S hydrochloride (15205), doxycycline hyclate (D9891), propidium iodide (P4170) and N-Ethylmaleimide (128-53-0) were obtained from Sigma Aldrich. GDC-0349 (S8040) and bortezomib (S1013) were obtained from Selleckchem (Houston, TX, USA). Puromycin dihydrochloride (A11138-03) was obtained from Gibco (Grand Island, NY, USA).

### Cell culture

HEK293 and HEK293T cells were maintained in Dulbecco's Modified Eagle's Medium (Welgene, Gyeongsan, Republic of Korea) supplemented with 10% fetal bovine serum (FBS; Gibco). MCF7 cells were maintained in Minimum Essential Medium Eagle (MEM; Welgene) and HT29 cells in McCoy's 5A Modified Medium (Gibco), which were all supplemented with 10% FBS. All cell lines confirmed to be mycoplasma free using Mycoplasma PCR Detection Kit (25235, iNtRON Biotechnology, Seongnam, Republic of Korea). Lentivirus production, transduction, cell lysis, immunoprecipitation, and immunoblotting were performed as previously described [10].

### Plasmids and transfection

pCMV-Sport6-mouse OTUD5 (NCBI accession number: NM\_138604.3) clone was provided from Korea Human Gene Bank, KRIBB (Daejeon, Republic of Korea). Myc-mTOR was a kind gift from David Sabatini [11] (Addgene plasmid #1861). shRNAs were cloned into TRC2 pLKO.5-puro vectors (SHC202, Sigma Aldrich) or EZ-Tet-pLKO-Hygro vector (a kind gift from Cindy Miranti [12] (Addgene plasmid #85973)). Small guide RNA (sgRNA) targeting OTUD5 was constructed into pL-CRISPR.SFFV.tRFP vector [13] (a kind gift from Benjamin Ebert (Addgene plasmid # 57826)). The sequences of oligos corresponding to shRNAs and sgRNAs are listed in

Supplementary Table S2. Cells were transfected with various plasmids using X-treamGENE™ HP DNA Transfection Reagent (Roche) according to the manufacturer's instructions.

Small interfering RNAs (siRNAs) against TSC1 (1156989),  $\beta$ TrCP1 (1013833),  $\beta$ TrCP2 (1051953), and negative control siRNA (SN-1003) were purchased from Bioneer (Daejeon, Republic of Korea). siRNAs against OTUD5 (L-013823-00) were obtained from Dharmacon (Lafayette, CO, USA). The cells were transfected with various siRNAs using Lipofectamine RNAiMAX Reagent (Invitrogen, Carlsbad, CA, USA) according to the manufacturer's instruction. After 48–72 h incubation, the cells were harvested and analyzed.

### Quantitative real-time polymerase chain reaction (real-time qPCR) analysis

Total RNA was extracted from cells using an RNeasy Plus Mini Kit (QIAGEN, Hilden, Germany) and 2  $\mu$ g of total RNA was reverse transcribed using a RevertAid H Minus First Strand cDNA Synthesis Kit (Thermo Fisher Scientific) according to the manufacturer's protocol. Real-time qPCR was performed using Solg 2X Real-Time PCR Smart mix (SolGent, Daejeon, Republic of Korea) and gene-specific primers (Supplementary Table S3). The human GAPDH gene was used for normalization.

### In vitro mTOR kinase assay

HEK293T cells transfected with Myc-mTOR wild type and KD, respectively, were lysed using CHAPS lysis buffer (40 mM HEPES, pH 7.4, 120 mM NaCl, 2 mM EDTA, 0.3% CHAPS, 10 mM sodium pyrophosphate, 10 mM  $\beta$ -glycerophosphate disodium salt, 50 mM NaF) containing protease inhibitors. The clarified lysates were immunoprecipitated with anti-c-Myc magnetic beads at 4 °C for 3 h. The beads were washed three times with CHAPS lysis buffer, and then once with wash buffer (CHAPS lysis buffer with 500 mM NaCl). The Myc-OTUD5 proteins were immunoprecipitated using anti-c-Myc magnetic beads. In the final washing step, the Myc-OTUD5 and Myc-mTOR immune complexes were combined and washed once with kinase wash buffer (25 mM HEPES-KOH, pH 7.4 and 20 mM KCl). The kinase assay was performed by adding mTOR kinase reaction buffer (25 mM HEPES, pH 7.4, 50 mM KCl, 10 mM MgCl<sub>2</sub>, 250  $\mu$ M ATP, 10  $\mu$ Ci [ $\gamma$ -<sup>32</sup>P] ATP) and incubating at 30 °C for 30 min. In the experiment using recombinant OTUD5, 2  $\mu$ g recombinant OTUD5 was added to the kinase reaction buffer. The reactions were stopped with the addition of Laemmli buffer. The proteins were separated using SDS-PAGE and stained with InstantBlue™ Protein Gel Stain (Expedeon, San Diego, CA,

USA). After drying the stained gel on Whatman 3MM paper, <sup>32</sup>P incorporation was determined by film exposure.

### Identification of OTUD5 phosphorylation sites

Murine OTUD5 proteins purified from *E. coli* (10  $\mu$ g) were incubated with or without mTOR wild type or KD mutant precipitates in mTOR kinase reaction buffer (without [ $\gamma$ -<sup>32</sup>P] ATP) at 30 °C for 2 h as described in the In Vitro mTOR Kinase Assay subsection of the “Materials and methods” section. The reactants were separated via SDS-PAGE. The gel was stained with Coomassie blue so that the OTUD5 bands could be visualized for gel excision. The phosphopeptides from the OTUD5 bands were analyzed by BioCon (Seoul, Republic of Korea) using liquid chromatography-mass spectrometry.

### Flag-OTUD5 purification from mammalian cells

HEK293T cells were transfected with pcDNA3.1-Flag-OTUD5-wild type, -S177A, and -3SA mutant constructs. After 72 h incubation, the cells were lysed and the Flag-OTUD5 proteins were immunoprecipitated with anti-DYKDDDDK magnetic beads. The immune complexes were incubated at 4 °C for 6 h with Flag elution buffer (25 mM HEPES, pH 7.5, 50 mM NaCl, 1 mM EDTA, 10% glycerol, 250  $\mu$ g 3  $\times$  Flag peptide [Sigma Aldrich], phosphatase inhibitor cocktail [Roche]) without protease inhibitor to elute the bound proteins from the beads. Then, the protein concentration was determined by the Bradford method.

### In vitro DUB assay

Various types of Flag-OTUD5 proteins (100 nM) were reacted with 1  $\mu$ M Ub-AMC (Boston Biochem, Cambridge, MA, USA) in DUB buffer (50 mM Tris-HCl, pH 8.0, 100 mM NaCl, 1% glycerol, 5 mM DTT) at room temperature. The sample's fluorescence was read at an excitation wavelength of 345 nm and an emission wavelength of 445 nm every 10 min for 2 h in VICTOR™ X Multilabel Plate Reader (PerkinElmer, Waltham, MA, USA).

### RNA sequencing

Total RNA was extracted from *OTUD5*<sup>+/+</sup>, *OTUD5*<sup>-/-</sup>, and GDC-0349-treated HEK293 cells in duplicates. An RNA sequencing library was prepared using the TruSeq RNA Sample Prep Kit v2 (Illumina, San Diego, CA, USA), and sequencing was performed on an Illumina HiSeq 2000 sequencing platform to generate 100-bp paired-end reads. The sequenced reads were mapped to the human genome (hg19) using STAR 2.5.1 software [14], and the gene expression levels were quantified with the count

module in STAR. The edgeR 3.12.1 [15] package was used to select DEGs from the RNA-seq count data<sup>24</sup>. Meanwhile, the trimmed mean of M-values normalized counts per million value of each gene was floored to one and log<sub>2</sub>-transformed for further analysis.

### Gene set enrichment analysis

We utilized GSEA 3.0 software ([www.broadinstitute.org/gsea/index.jsp](http://www.broadinstitute.org/gsea/index.jsp)) to study specific groups of genes according to the default parameters [16]. We used the Hallmark gene collection from the predefined Molecular Signatures Database gene set (MsigDB; <http://software.broadinstitute.org/gsea/msigdb/index.jsp>) to determine whether the predefined gene sets were enriched in the observed gene expression profile. The genes were ranked according to the significant differences in expression that were observed among three conditions (*OTUD5*<sup>+/+</sup>, *OTUD5*<sup>-/-</sup>, and GDC-0349) in the gene expression data. Given the MSigDB gene set, an enrichment score (ES) was calculated to measure the overrepresentation of members of that gene set appearing at the extremes (up- or down-regulation) of the ranked gene list. The ES was then evaluated for significance using gene-based permutation tests. The ES, together with the permutation *P*-value, indicated the degree to which the defined gene was enriched in the gene expression data. The comparison conditions between the groups were set as *OTUD5*<sup>+/+</sup> vs. *OTUD5*<sup>-/-</sup>, *OTUD5*<sup>+/+</sup> vs. GDC-0349, and *OTUD5*<sup>+/+</sup> vs. REST (*OTUD5*<sup>-/-</sup>, GDC-0349).

### Data access

The next-generation sequencing data were deposited in the NCBI Gene Expression Omnibus accession number: GSE135078. The raw sequence tags were deposited in the NCBI Sequence Read Archive (SRA) accession number: SRP216807.

### Cell size measurement

Trypsin-EDTA was used to harvest  $2 \times 10^6$  cells in 60-mm culture dishes. Then, the cells were resuspended in 10% FBS/phosphate-buffered saline (PBS). After centrifugation at  $200 \times g$  for 3 min, the cells were washed once with 1% FBS/PBS, and the pellets were resuspended in 75% ethanol/PBS and incubated at 4 °C for 12 h for fixation. The fixed cells were centrifuged at  $200 \times g$  for 3 min and washed once with 1% FBS/PBS. Thereafter, they were incubated with 1% FBS/PBS containing 0.1% Triton X-100 and 250 µg/ml RNase A at 37 °C for 30 min. After incubation, the cells were stained with 20 µg propidium iodide and analyzed by fluorescence-activated cell sorting.

### Fly stocks used

Following fly stocks were obtained from Vienna *Drosophila* Resource Center (Vienna, Austria): *UAS-Duba RNAi* (v27588), *UAS-Duba RNAi* (v27589), and *UAS-Duba RNAi* (v109912). *UAS-Rheb* (BL9688) was obtained from Bloomington *Drosophila* Stock Center (Bloomington, IN, USA). *ap-Gal4* was kindly provided by Prof. J. Chung (Seoul National University, Republic of Korea).

### Immunofluorescence microscopy

HeLa cells were seeded in µ-Slide 8-well chamber slides (#80826, Ibidi, Gräfelfing, Germany) at a density of  $5 \times 10^4$  cells/well. The following day, the cells were washed with warm PBS and then fixed in 4% paraformaldehyde in PBS for 20 min at room temperature. After a wash-out with PBS, the cells were mounted in Fluoroshield Mounting Medium with DAPI (ab104139, Abcam). The fluorescence signals were measured using a ZEISS LSM 880 laser scanning microscope.

### Proliferation assay

A cell proliferation assay was performed using a CellTiter-Glo® Luminescent Cell Viability Assay Kit (Promega, Madison, WI, USA) according to the manufacturer's protocol.

### Statistical analysis

All experiments were performed in replicate or triplicate and representative results were presented where data were expressed as mean ± SD mentioned in figure legends. Variance between groups statistically compared was similar. All statistical analyses were carried out using Microsoft Excel program. Two-tailed student's *t* test was used to compare the difference between groups.

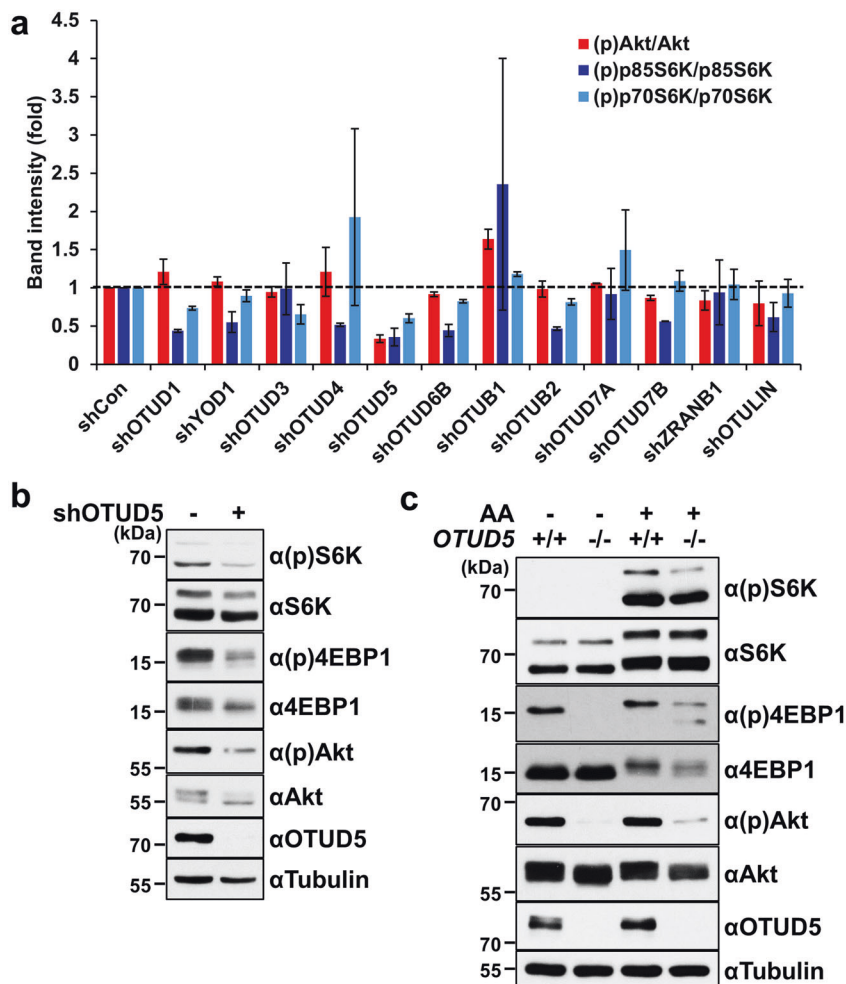
## Results

### OTUD5 is a positive regulator of mTORC1 and mTORC2 signaling pathways

To identify DUBs that were involved in mTORC1 and mTORC2 signaling pathways, we examined the activity of mTOR signaling using HEK293 stable cell lines that expressed short hairpin RNAs (shRNAs) targeting 15 DUBs of the OTU family. Among the 11 DUBs where the expression level was reduced by >50% compared with that of the control cells (Supplementary Fig. S1), OTUD5

**Fig. 1 OTUD5 is required for both the mTORC1 and mTORC2 signaling pathways.**

**a** Quantification of the band intensity of phosphorylated Akt and S6K from Supplementary Fig. S2. The phosphorylation level of Akt and S6K was normalized with total Akt and S6K, respectively. **b** Whole-cell extracts from HEK293 cells stably expressing control (shCon) or OTUD5 shRNA (shOTUD5) were analyzed by immunoblotting to assess the levels of the indicated proteins and phosphorylation. **c** *OTUD5* wild-type (*OTUD5*<sup>+/+</sup>) or CRISPR/Cas9-edited *OTUD5* knockout (*OTUD5*<sup>-/-</sup>) HEK293 cells were subjected to amino acid starvation for 3 h and resupplementation for 1 h.



was the only DUB where the knockdown significantly reduced the phosphorylation of 4EBP1 at Thr37/46, S6K at Thr389, and Akt at Ser473, which are the representative phosphorylation sites of mTORC1 and mTORC2 (Fig. 1a, b; Supplementary Fig. S2). Moreover, the OTUD5 depletion reduced the phosphorylation of mTORC1/2 substrates in HT29 colon cancer cell line (Supplementary Fig. S2m), indicating that this phenomenon is not limited to HEK293 cells. In line with this, CRISPR/Cas9-mediated deletion of *OTUD5* (Supplementary Fig. S3a) recapitulated this phenotype (Fig. 1c). These data suggested that OTUD5 played an important role in the mTOR pathway.

**OTUD5 modulates the protein stability of DEPTOR, an inhibitory subunit of mTORCs**

To elucidate how OTUD5 simultaneously regulated mTORC1/2 signaling, we examined the protein abundance of the mTOR complex subunits, such as mTOR, GβL, and

DEPTOR, which are commonly found in both mTORC1 and mTORC2 [1]. It was intriguing that the protein level of DEPTOR, an inhibitory subunit of mTORC1 and mTORC2 [17], was dramatically increased in OTUD5-depleted HEK293 cells and HT-29 cells (Fig. 2a, d; Supplementary Fig. S3b, c), while its mRNA level remained constant (Fig. 2b). Meanwhile, there was no change in the amount of mTOR, GβL, and tuberous sclerosis complex (TSC) 1/2 (Fig. 2a). In accordance with this, the ectopic expression of OTUD5 in HEK293T led to a reduced protein level of DEPTOR (Fig. 2c). The increase in the level and half-life of DEPTOR in OTUD5-depleted cells was restored by re-expression of OTUD5 (Fig. 2d; Supplementary Fig. S3d, e), ruling out the possibility of the off-target effect of the gene silencing. Furthermore, knockdown of the elevated DEPTOR in OTUD5-depleted cells reactivated the mTORC1 and mTORC2 pathways (Fig. 2e). These results suggested that OTUD5 acted as a positive regulator in mTORC1 and mTORC2 signaling by modulating the protein abundance of DEPTOR.

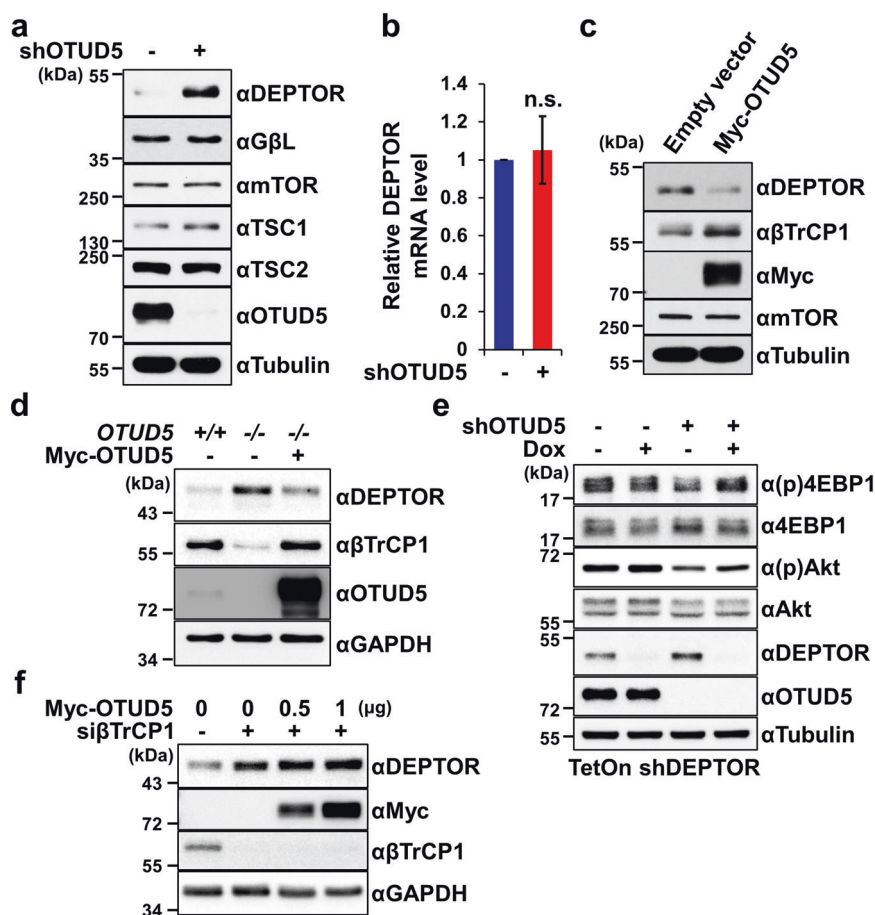


**Fig. 2 OTUD5 modulates mTOR signaling via regulating the protein stability of DEPTOR.** **a** Whole-cell lysates from HEK293 cells stably expressing shCon or shOTUD5 were subjected to immunoblotting with the indicated antibodies. **b** The DEPTOR mRNA level was analyzed by real-time qPCR in HEK293 shCon or shOTUD5 stable cell lines. These data represent means  $\pm$  SD of three experiments. n.s., not significant. **c, d** HEK293T (**c**) and *OTUD5*<sup>+/+</sup> or *OTUD5*<sup>-/-</sup> HEK293 (**d**) cells were transfected with an empty vector or Myc-OTUD5. Whole-cell extracts were subjected to western blotting with the indicated primary antibodies. **e** HEK293 cells stably

expressing doxycycline-inducible shRNA targeting DEPTOR were transfected with lentiviral shCon or shOTUD5. After selection with puromycin for 72 h, the cells were further incubated in the absence or presence of 1  $\mu$ g/ml doxycycline for 72 h. The phosphorylation status and protein level were analyzed via immunoblotting. **f** HEK293 cells were transfected with siRNA control or targeting  $\beta$ TrCP1 and the indicated amount of Myc-OTUD5 construct. After 48 h incubation, whole-cell extracts were subjected to immunoblotting with the indicated antibodies.

### OTUD5 stabilizes $\beta$ TrCP1 by removing the ubiquitin chains on $\beta$ TrCP1, leading to DEPTOR degradation

The phosphorylated DEPTOR by mTOR, CK1 $\alpha$ , and p90 ribosomal protein S6 kinase 1 (p90RSK1) is recognized and polyubiquitinated by the Skp1, Cullin1, and F-box <sup>$\beta$ TrCP</sup> (SCF <sup>$\beta$ TrCP</sup>) E3 ligase complex and rapidly degraded [18–20]. According to these reports, we hypothesized that OTUD5 might deubiquitinate and stabilize  $\beta$ TrCP, subsequently modulating DEPTOR. Overexpression of OTUD5 increased  $\beta$ TrCP1 proteins (Fig. 2c), whereas OTUD5 depletion significantly reduced the abundance and the half-life of  $\beta$ TrCP1 protein without any significant change in  $\beta$ TrCP1 mRNA level (Fig. 2d; Supplementary Fig. S3c, g, h). The decrease level and half-life of  $\beta$ TrCP1 were restored by the ectopic

expression of OTUD5 (Fig. 2d; Supplementary Fig. S3d, e). A simultaneous decrease in the level of  $\beta$ TrCP1/2 elicited an increase in DEPTOR and inhibition of the mTOR pathway [18–20] (Supplementary Fig. S3f). However, OTUD5 overexpression in the  $\beta$ TrCP1-depleted cells failed to reduce DEPTOR (Fig. 2f). These data suggested that OTUD5 regulates the abundance of DEPTOR via stabilizing  $\beta$ TrCP1.

Next, we investigated the mechanisms of the OTUD5-mediated stabilization of  $\beta$ TrCP1. Bortezomib, a proteasome inhibitor, restored the reduced level of  $\beta$ TrCP1 in OTUD5-depleted cells (Fig. 3a, b), indicating that  $\beta$ TrCP1 was degraded through proteasomes by OTUD5 depletion. Because OTUD5 belongs to the DUB family, it was plausible that  $\beta$ TrCP1 was a substrate for OTUD5. Through a reciprocal co-immunoprecipitation (co-IP) assay, the interaction between

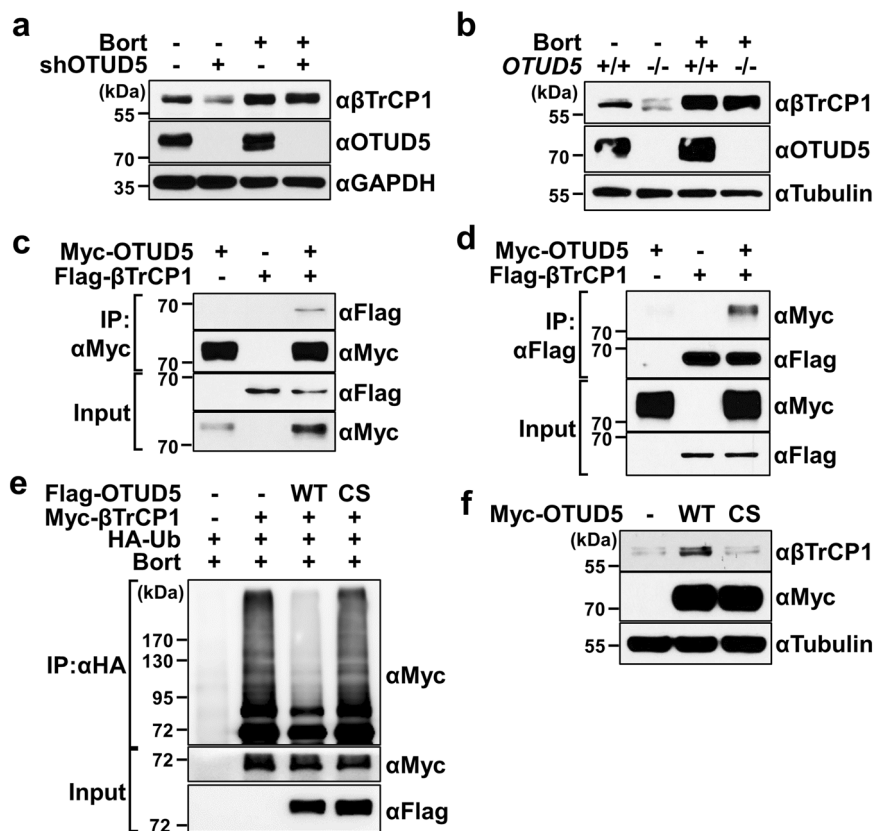


**Fig. 3 OTUD5 deubiquitinates and stabilizes  $\beta\text{TrCP1}$ .** **a, b** HEK293 cells stably expressing shCon or shOTUD5 (**a**) and *OTUD5*<sup>+/+</sup> or *OTUD5*<sup>-/-</sup> HEK293 cells (**b**) were treated with DMSO or 1  $\mu\text{M}$  bortezomib (Bort) for 12 h. **c, d** HEK293T cells were co-transfected with empty vector, Myc-OTUD5, or Flag- $\beta\text{TrCP1}$  as indicated. After 48 h, Myc-OTUD5 (**c**) or Flag- $\beta\text{TrCP1}$  (**d**) were immunoprecipitated and analyzed by immunoblotting with the indicated antibodies to detect OTUD5 and  $\beta\text{TrCP1}$  interaction. **e** HEK293T cells were transiently transfected with empty vector or

Flag-OTUD5 wild type (WT), C224S mutant (CS), and Myc- $\beta\text{TrCP1}$  and HA-tagged-ubiquitin (HA-Ub) as indicated. After bortezomib treatment, HA-Ub was immunoprecipitated and analyzed by immunoblotting with the indicated antibodies to assess the amount of ubiquitination of Myc- $\beta\text{TrCP1}$ . **f** HEK293T cells were transfected with empty vector, Myc-OTUD5 WT, or CS mutant. Whole-cell extracts were subjected to immunoblotting with the indicated primary antibodies.

OTUD5 and  $\beta\text{TrCP1}$  in the cells was confirmed (Fig. 3c, d). Moreover, the ubiquitination of  $\beta\text{TrCP1}$  was markedly reduced upon the ectopic expression of OTUD5 wild-type, but not the catalytic mutant (C224S; the numbering is hereafter based on murine OTUD5 amino acid sequence) (Fig. 3e; Supplementary Fig. S3i). Also, OTUD5 C224S overexpression did not increase the endogenous  $\beta\text{TrCP1}$  protein compared with the OTUD5 wild-type (Fig. 3f). Taken together, these data demonstrated that OTUD5 deubiquitinated and stabilized  $\beta\text{TrCP1}$  via its DUB activity.

To further elucidate the molecular mechanism, we attempted to map the interaction domain of OTUD5 with  $\beta\text{TrCP1}$ . OTUD5 contains the catalytic OTU domain and the ubiquitin-interacting motif (UIM) [8]. Through co-IP, the UIM domain-containing OTUD5 fragment was found to strongly interact with  $\beta\text{TrCP1}$  but the OTU domain-containing one was not (Supplementary Fig. S4a). In case of  $\beta\text{TrCP1}$ , it consists of F-box domain and WD40 repeats

[21], WD40 repeats containing-truncation mutant was found to interact with OTUD5 but not F-box containing-mutant (Supplementary Fig. S4b). It was reported that two residues in UIM domain are essential for the interaction with ubiquitin chains [8]. The substitution of Leu537/Ser544 to Ala in murine OTUD5 construct led to a failure of the interaction with  $\beta\text{TrCP1}$  (Supplementary Fig. S4c), indicating that the ubiquitin chains of  $\beta\text{TrCP1}$  might mediate the OTUD5- $\beta\text{TrCP1}$  interaction. Indeed, the interaction between OTUD5 and  $\beta\text{TrCP1}$  was markedly increased by the proteasome inhibitor treatment and the ectopically expressed OTUD5 C224S mutant which enhanced the  $\beta\text{TrCP1}$  ubiquitination (Supplementary Fig. S4d). In addition, another catalytic mutant, S177A, also strongly interacted with  $\beta\text{TrCP1}$  compared with wild-type OTUD5 (Supplementary Fig. S4e). However, bacterially purified  $\beta\text{TrCP1}$  and OTUD5 wild-type or C224S mutant, which do not have posttranslational modifications, failed to bind to

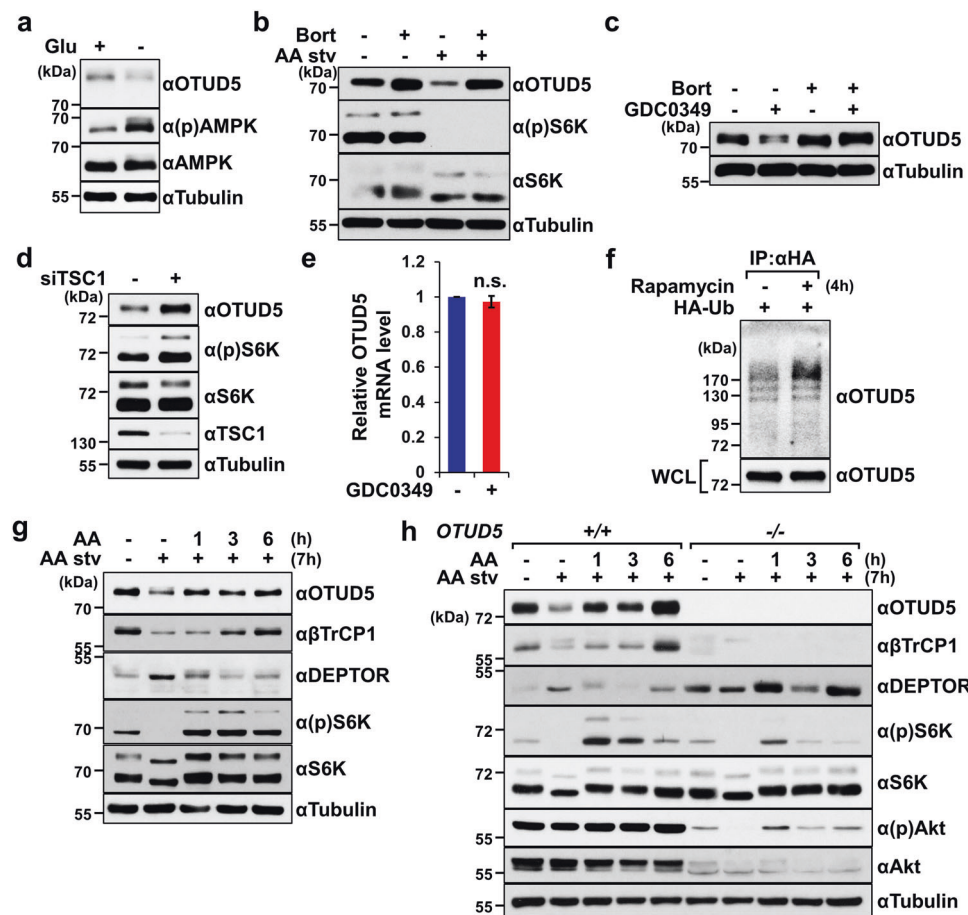


**Fig. 4 mTOR activity is required for OTUD5 stability.** **a** Whole-cell lysates from HEK293 cells that were glucose-starved for 5 h were analyzed by immunoblotting with the indicated antibodies. **b** HeLa cells were amino acid-starved (AA stv) with Dulbecco's phosphate-buffered saline (DPBS) for 5 h in the presence of DMSO or 1  $\mu$ M bortezomib. Whole-cell lysates were analyzed by immunoblotting with the indicated antibodies. **c** HEK293 cells were treated with DMSO or 1  $\mu$ M GDC-0349 for 12 h in the presence of DMSO or 1  $\mu$ M bortezomib. **d** Whole-cell extracts from HEK293 cells transfected with control or TSC1 siRNA (siTSC1) for 48 h were subjected to immunoblotting. **e** OTUD5 mRNA levels were analyzed by real-time qPCR

in HEK293 cells treated with DMSO or 1  $\mu$ M GDC-0349 for 12 h. These data represent means  $\pm$  SD of two independent experiments. n.s.: not significant. **f** HEK293T cells transfected with HA-Ub were treated with DMSO or 100 nM rapamycin for 4 h. HA-Ub was immunoprecipitated with HA-antibody and analyzed by immunoblotting. WCL: whole-cell lysate. **g, h** HEK293 cells (**g**) and *OTUD5*<sup>+/-</sup> or *OTUD5*<sup>-/-</sup> HEK293 cells (**h**) were amino acid-starved with DPBS (AA stv) and stimulated with complete growth medium (AA) for the indicated hours. Whole-cell extracts were subjected to immunoblotting with the indicated primary antibodies.

each other (Supplementary Fig. S4f). Taken together, these data demonstrated that OTUD5 interacted with the ubiquitin chains of  $\beta$ TrCP1 via UIM.

$\beta$ TrCP1 has been known to recognize various phosphoproteins, including  $\beta$ -catenin as well as DEPTOR, enabling it to negatively regulate the wingless-related integration site (Wnt) pathway [22, 23]. The depletion of OTUD5 enhanced Wnt3A-induced luciferase reporter activity (Supplementary Fig. S5a). Moreover, GDC-0349, an mTOR kinase inhibitor, augmented Wnt3A-induced reporter activity (Supplementary Fig. S5b). Furthermore, *Duba* RNA interference (RNAi) in *Drosophila* wing disc enhanced the expression of *Armadillo*, a fly ortholog of  $\beta$ -catenin and one of the target

genes of the *Wingless* pathway (Supplementary Fig. S5c, d). Collectively, we demonstrated that OTUD5 deubiquitinated and stabilized  $\beta$ TrCP1 in vivo.

### mTOR activity is required for the stability of OTUD5

Interestingly, on investigating the roles of OTUD5 in mTOR signaling, we found out that the amount of OTUD5 protein changed according to the amino acid availability (Fig. 1c). The protein level of OTUD5 was reduced when mTOR was inhibited by nutrient starvation (Fig. 4a, b; Supplementary Fig. S6a) or its inhibitors, rapamycin and GDC-0349 (Fig. 4c; Supplementary Fig. S6b, c).



Conversely, when mTOR was activated by TSC1 knock-down, the OTUD5 level was elevated (Fig. 4d). While GDC-0349 did not affect the mRNA level of OTUD5 (Fig. 4e), rapamycin increased the ubiquitination of OTUD5 *in vivo* (Fig. 4f; Supplementary Fig. S6d). In addition, the proteasome inhibitor restored the level of OTUD5 proteins suppressed by the inhibition of mTOR (Fig. 4b, c). Collectively, these data showed that the stability of OTUD5 was post-translationally regulated by mTOR activity.

Next, we found out that the inactivation of mTOR by nutrient deprivation markedly decreased  $\beta$ TrCP1 as well as OTUD5 and increased DEPTOR (Fig. 4g). Conversely, the activation of mTOR by amino acids and glucose increased the protein level of  $\beta$ TrCP1 as well as OTUD5 and decreased DEPTOR (Fig. 4g). However, the mTOR activation by nutrients did not increase  $\beta$ TrCP1 in OTUD5 depleted cells and as a result failed to decrease the DEPTOR protein (Fig. 4h). These data demonstrated that mTOR was able to modulate  $\beta$ TrCP1-mediated DEPTOR degradation via OTUD5.

### mTOR directly phosphorylates and regulates the DUB activity of OTUD5

Since the level of OTUD5 appeared to be correlated with mTOR activity, we speculated that mTOR might directly phosphorylate OTUD5. Incubation with lambda phosphatase caused the multiple bands of the immunoprecipitated OTUD5 to migrate faster on an SDS-PAGE gel, suggesting that OTUD5 was indeed a phosphoprotein (Supplementary Fig. S7a). Next, in an *in vitro* mTOR kinase assay, mTOR wild-type, but not kinase-dead (KD) mutant, phosphorylated ectopically expressed or bacterially purified OTUD5 (Fig. 5a; Supplementary Fig. S7b). To identify the phosphorylation sites of OTUD5, we conducted mass spectrometry analysis using bacterially purified murine OTUD5 proteins incubated with mTOR, which resulted in the identification of seven different phosphorylation sites: Thr195, Ser323, Ser332, Ser370, Ser447, Thr502, and Ser503 (Supplementary Fig. S7c). Among these sites, the substitution of Ser323, Ser332, or Ser503 to Ala partially reduced phosphorylation, and a simultaneous mutation of all of three residues almost abolished phosphorylation (Fig. 5b; Supplementary Fig. S7d). Ser323 and Ser332 were located flanking the His329 and Asn331 residues of the catalytic triad [24] and Ser503 was located near the UIM of OTUD5 (Supplementary Fig. S7e). These serines are evolutionarily conserved in vertebrates (Supplementary Fig. S7f). To confirm these results, an antibody that recognized the phosphorylated Ser503 of OTUD5 was generated. The specificity of the antibody was validated by dot blot analysis (Supplementary Fig. S7g). Indeed, Ser503

phosphorylation of OTUD5 was elevated upon stimulation with amino acids (Fig. 5c) and conversely abolished by amino acid starvation and GDC-0349 treatment (Fig. 5c, d).

Next, we showed that mutations at Ser323/332 and Ser323/332/503 (3SA) of OTUD5 resulted in a significant increase in its ubiquitination (Fig. 5e; Supplementary Fig. S8a). In addition, bortezomib restored the lower protein level of 3SA OTUD5 to that of the wild-type (Fig. 5f). Furthermore, the half-life of 3SA mutants was shorter than that of the wild-type (Supplementary Fig. S8b), suggesting that the phosphorylation by mTOR might impede the ubiquitination of OTUD5.

To test whether the phosphorylation by mTOR modulated the DUB activity of OTUD5, we conducted an *in vitro* DUB assay as described in “Materials and methods”. The DUB activity of OTUD5 from GDC-0349-treated cells was lower than that of control (Fig. 5g). Furthermore, the 3SA mutants demonstrated less DUB activity than the wild-type (Fig. 5h). In addition, the mTOR inhibition by GDC-0349 or rapamycin treatment increased the ubiquitination of  $\beta$ TrCP1 (Supplementary Fig. S8c, d) and TRAF3 (Supplementary Fig. S8e, f). In line with this, the OTUD5 3SA mutant showed reduced DUB activity against the polyubiquitin chains of  $\beta$ TrCP1 (Fig. 5i; Supplementary Fig. S8g–i) and TRAF3 (Supplementary Fig. 8j, k).

Then, we tested whether the interaction between OTUD5 and  $\beta$ TrCP1 was regulated by mTOR activity in physiological condition. Under the proteasome inhibitor, we observed that the activation of mTOR by amino acids dramatically reduced the physical interaction between endogenous OTUD5 and  $\beta$ TrCP1 (Fig. 5j). Taken together, these data demonstrated that the mTOR-mediated phosphorylation at Ser323/332/503 activated the DUB activity of OTUD5 and consequently stabilized  $\beta$ TrCP1.

### OTUD5 regulates the downstream pathways of mTORC1 and mTORC2

To investigate whether OTUD5 affects cellular processes downstream of mTOR, we performed RNA sequencing (RNA-seq) analysis and identified differentially expressed genes (DEGs) across OTUD5 wild-type-, OTUD5 null- and GDC-0349 treated-HEK293 cells (fold change >2; false discovery rate FDR  $q$  value < 0.05) (Supplementary Fig. S9a). Then, we performed Gene Set Enrichment Analysis (GSEA) on the DEGs using a collection of 50 hallmark gene sets from comparisons between OTUD5 wild-type cells and REST (both OTUD5 null cells and GDC-0349 treated cells). A comparison between OTUD5 wild-type and OTUD5 null cells showed significant changes of expression in the genes involved in pathways that had been previously

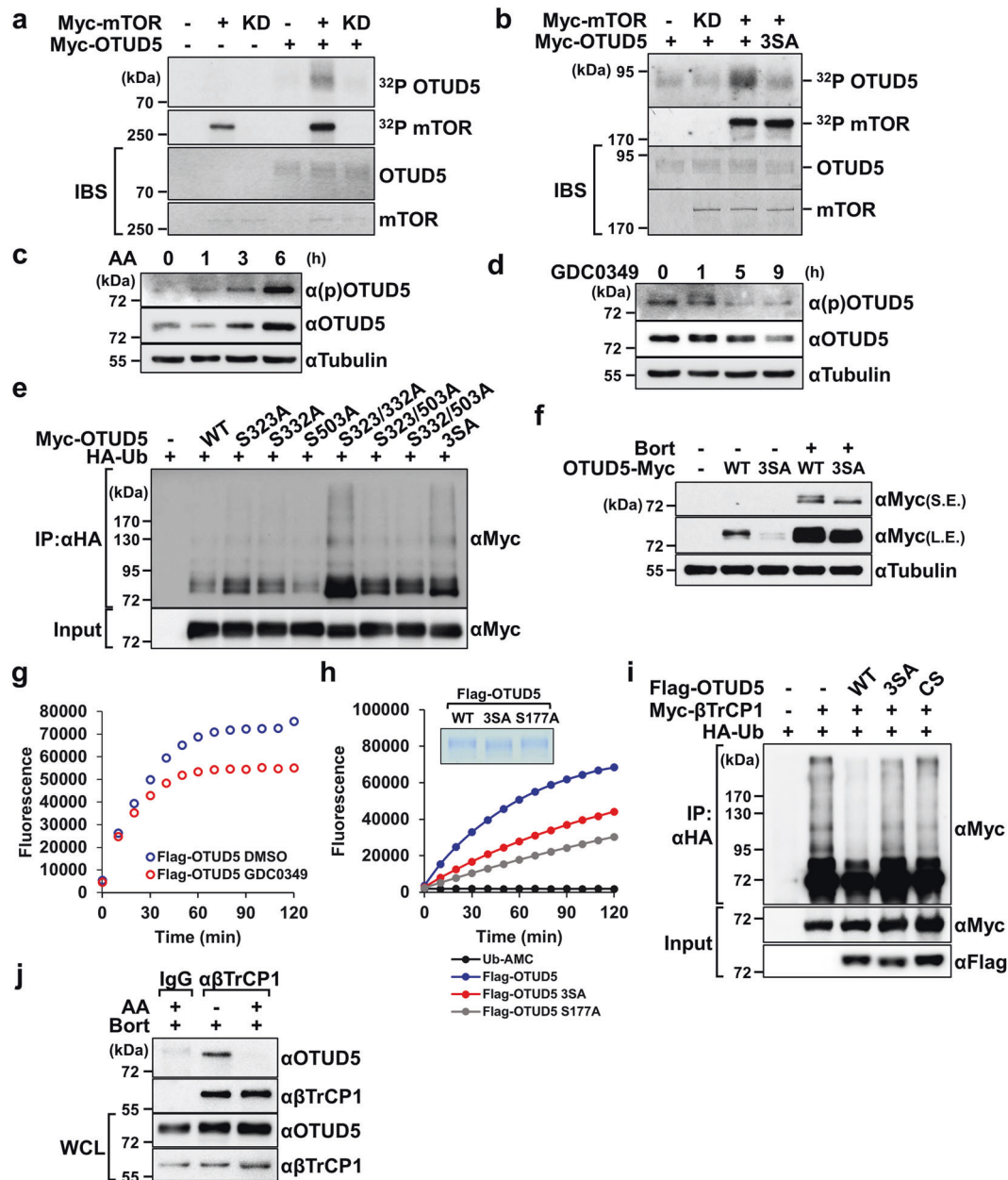


**Fig. 5 mTOR directly phosphorylates and regulates the DUB activity of OTUD5.** **a, b** In vitro kinase assay using Myc-OTUD5 (**a**) or 3SA mutant (**b**) and Myc-mTOR wild-type or kinase-dead (KD) mutant as described in the Materials and Methods section. The upper two panels show  $^{32}\text{P}$ -incorporated OTUD5 and mTOR, and the lower two panels show the input amounts of OTUD5 and mTOR. **c** HEK293T cells that were amino acid-starved with DPBS for 1 h were stimulated with complete growth medium (AA) for the indicated times. Whole-cell extracts were analyzed by immunoblotting with the indicated antibodies. **d** HEK293T cells were treated with DMSO or 1  $\mu\text{M}$  GDC-0349 for the indicated times. Whole-cell lysates were subjected to immunoblotting with the indicated primary antibodies. **e** HEK293T cells were co-transfected with various constructs of Myc-OTUD5 and HA-Ub. HA-Ub was immunoprecipitated and analyzed with the indicated antibodies. **f** HEK293T cells were transfected with C-terminal Myc-tagged-OTUD5 wild type or 3SA mutant for 48 h. After 12 h of DMSO or 1  $\mu\text{M}$  bortezomib treatment, the cells were

lysed and analyzed by immunoblotting with the indicated antibodies. **g, h** In vitro DUB assay using Flag-OTUD5 purified from DMSO-treated or GDC-0349-treated (1  $\mu\text{M}$ , 6 h) HEK293T cells (**g**) and Flag-OTUD5 wild-type, 3SA, and S177A mutants purified from HEK293T cells (the inset shows the protein input) (**h**) as described in the “Materials and methods” section. **i** HEK293T cells were co-transfected with the indicated constructs. HA-Ub was immunoprecipitated and analyzed by immunoblotting with the indicated antibodies. The cell lysates were subjected to direct immunoblot with same antibodies (Input). **j** HEK293 cells in the presence of bortezomib were amino acid-starved with DPBS. After 2 h the cells were stimulated with complete growth medium (AA) for 3 h. Endogenous  $\beta\text{TrCP1}$  was immunoprecipitated with  $\beta\text{TrCP1}$  antibody and analyzed by immunoblotting with the indicated antibodies. IBS: InstantBlue Staining, 3SA: Myc-OTUD5 S323/332/503A, CS: Myc-OTUD5 C224S, S.E.: short exposure, L.E.: long exposure, WCL: whole-cell lysate.

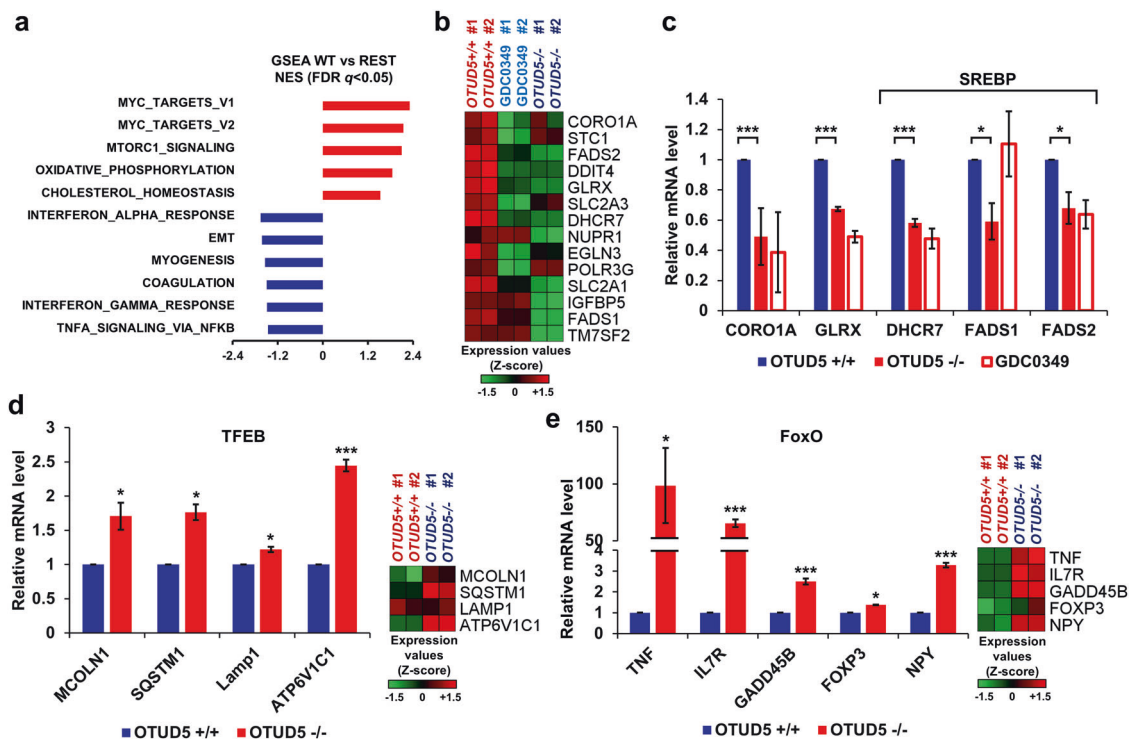


**Fig. 6** OTUD5 regulates the gene expression downstream of mTORC1 and mTORC2. **a** GSEA hallmark analysis of pathways significantly altered in OTUD5 wild-type versus REST (both OTUD5 null and GDC-0349 12-h-treated HEK293 cells). FDR  $q < 0.05$  for all pathways shown. **b** Heatmap showing DEGs of the mTORC1 signaling pathway signature gene set in OTUD5+/+ and OTUD5-/- and 1  $\mu$ M GDC-0349-treated (12 h) HEK293 cells.

**c–e** The mRNA levels of the indicated genes were analyzed by real-time qPCR in OTUD5+/+, OTUD5-/-, and 1  $\mu$ M GDC-0349-treated (12 h) HEK293 cells. These data represent means  $\pm$  SD of two experiments. Statistical analysis were performed using Microsoft Excel Student's *t* test, and *P* values  $< 0.05$  were considered significant (\* $P < 0.05$ , \*\*\* $P < 0.005$ ).

reported as associated with OTUD5 (Supplementary Fig. S9b). Using OTUD5 wild-type versus REST, we found that the expression of the genes involved in pathways of c-Myc and cholesterol homeostasis, as well as mTORC1 signaling were significantly altered (Fig. 6a). To validate the RNA-seq results, the expression of some of the core-enriched genes of the mTORC1 signaling pathway were analyzed using real-time qPCR. Consistent with the GSEA, the expression of *CORO1A*, *GLRX*, *DHCR7*, *FADS1*, and *FADS2* were significantly reduced in OTUD5 null and GDC-0349-treated HEK293 cells compared with OTUD5 wild-type cells (Fig. 6b, c).

mTOR controls the activities of transcription factors, such as sterol regulatory element-binding protein (SREBP), transcription factor EB (TFEB), and FoxO [1]. The expression of SREBP target genes, such as *DHCR7* and *FADS1/2*, was indeed downregulated in OTUD5 null cells (Fig. 6c). In addition, RNA-seq revealed that the target genes of TFEB and FoxO, which are negatively regulated by the mTORC1 and mTORC2 pathway, respectively [1], were upregulated in OTUD5 null cells (Fig. 6d, e; Supplementary Table S1). Taken together,

we demonstrated that OTUD5 regulated various cellular processes downstream of mTORC1 and mTORC2.

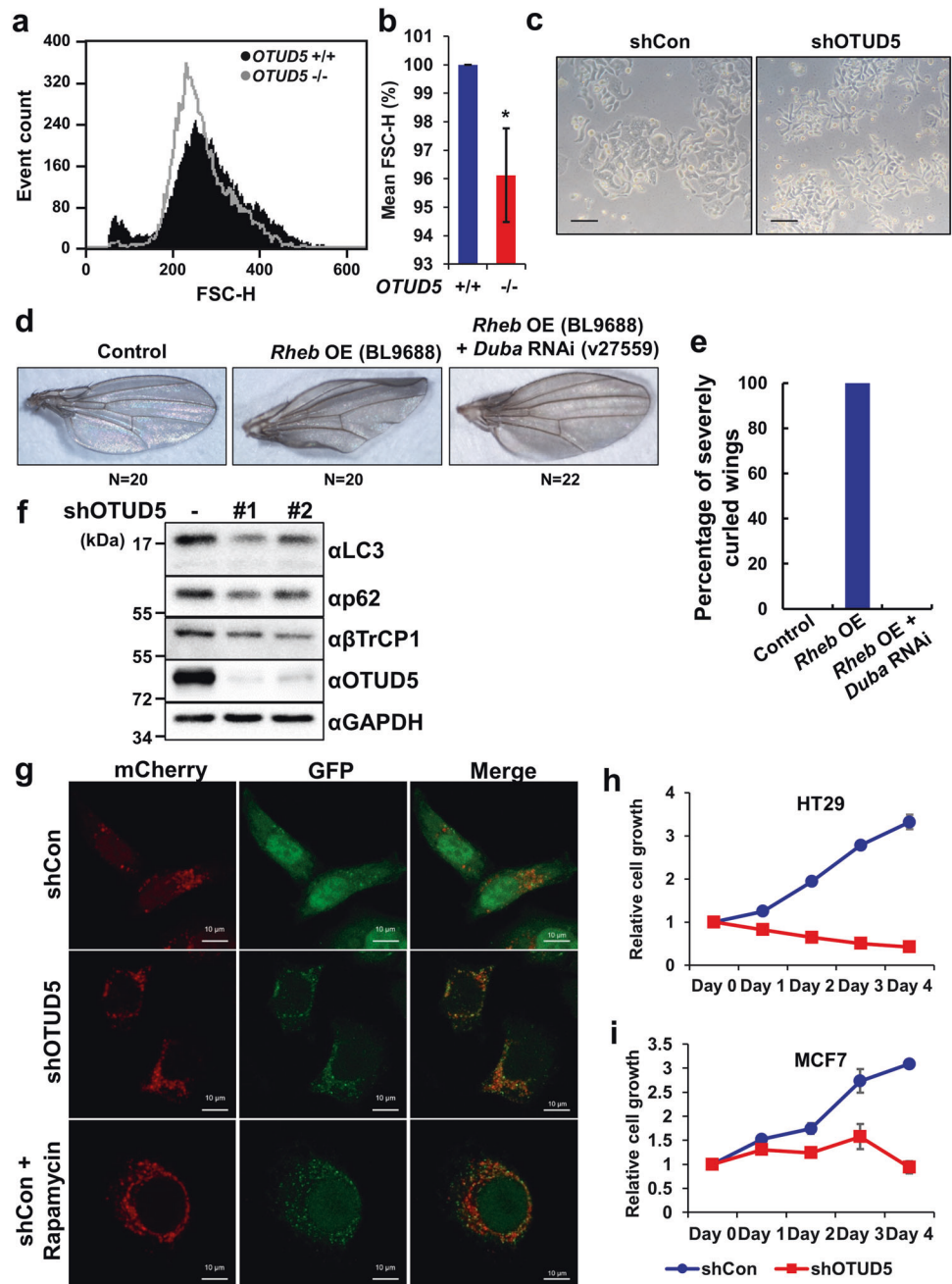
### OTUD5 regulates the cellular processes downstream of mTOR

Given that OTUD5 serves as a positive regulator of mTOR signaling, we examined the role of OTUD5 in cell growth, a key output of mTORC1 function [1, 25]. Compared to the wild-type cells, the mean values of cell size, decreased to ~4% in OTUD5-depleted HEK293 and HT29 cells (Fig. 7a–c; Supplementary Fig. S9c, d). Furthermore, it has been reported that the overexpression of *Drosophila Rheb* (*dRheb*), a positive regulator of *dTOR*, in the dorsal compartment of *Drosophila* wings results in the curled wing phenotype due to overgrowth of the compartment [26]. This phenotype was completely abolished by RNAi of *Duba*, the *Drosophila* ortholog of human OTUD5 (Fig. 7d, e), indicating that *Duba* was necessary to activate *dTOR* signaling downstream of *dRheb*.

Next, in both the OTUD5 knockdown and knockout cells, p62 (sequestosome 1) and LC3 proteins decreased compared

### Fig. 7 OTUD5 regulates the cellular processes downstream of mTORC1 and mTORC2.

**a, b** *OTUD5*<sup>+/+</sup> and *OTUD5*<sup>-/-</sup> HEK293 cells were analyzed by flow cytometry, as described in the Materials and Methods section, to determine the mean FSC-H. The mean FSC-H histograms are shown in **a**. Quantitation of triplicate experiments are shown in **b**. **c** Bright-field images of HT29 shCon (left) and shOTUD5 (right) cells used in Supplementary Fig. S9c, **d** (scale bar = 100  $\mu$ m). **d** Wings from wild type (left), *dRheb* overexpressed (*Rheb* OE) (middle), and *Rheb* OE with *Duba* RNAi (right) flies. *N* = number of flies. **e** Quantification of severely curled wings from **d** experiment. **f** Whole-cell lysates from HEK293 shCon and shOTUD5 stable cells were analyzed by immunoblotting with the indicated antibodies. **g** HeLa cells stably expressing mCherry-GFP-LC3B were infected with lentiviral shCon or shOTUD5 for 48 h and selected with puromycin for 72 h. After DMSO or rapamycin treatment (100 nM, 12 h), mCherry-GFP-LC3B were imaged by confocal microscopy as described in the Materials and Methods section (scale bar = 10  $\mu$ m). **h, i** HT29 (**h**) and MCF7 (**i**) cells were transduced with lentiviral shCon or shOTUD5 for 48 h and selected with puromycin for 48 h. Cell proliferation was assessed as described in the “Materials and methods” section.



with the control cells, indicating that autophagy had been augmented (Fig. 7f; Supplementary Fig. S9e). To further confirm the role of OTUD5 in autophagy, we utilized HeLa cells that stably expressed mCherry-GFP tandem-tagged-LC3B to measure autophagic flux [27]. Compared with the control cells that displayed a few red puncta (autolysosomes), the OTUD5-knockdown cells showed increased yellow puncta (autophagosomes) and red puncta, as seen in rapamycin-treated cells (Fig. 7g). These data indicated that OTUD5 suppressed autophagic flux via mTOR.

Since both mTORC1 and mTORC2 are able to be activated downstream of PI3K signaling, we examined whether OTUD5 affected the proliferation of cancer cells containing driver mutations in *PIK3CA*. Indeed, the OTUD5 depletion significantly inhibited the proliferation of HT29 (*PIK3CA* P449T) and MCF7 (*PIK3CA* E542K; E545K) cells [28] (Fig. 7h, i). These results suggested that OTUD5 downregulation might be a potential novel therapeutic approach in cancers showing active PI3K or mTOR signaling.

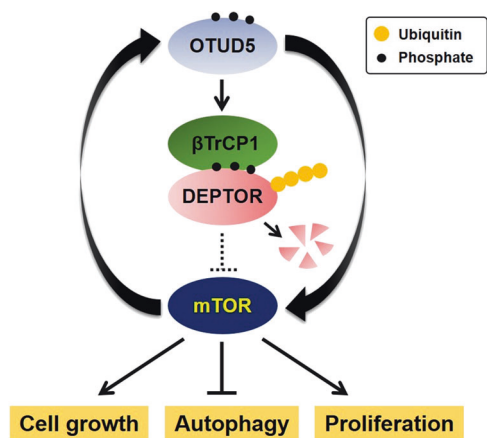


**Fig. 8 Schematic overview for the positive feedback loop between OTUD5 and mTOR signaling pathway.** OTUD5 stabilizes  $\beta$ TrCP1 through its DUB activity. In turn, the stabilized  $\beta$ TrCP1 degrades phosphorylated DEPTOR, an inhibitory subunit of mTOR complexes. The active mTOR directly phosphorylates and activates OTUD5 and promotes OTUD5- $\beta$ TrCP1-DEPTOR pathway. The positive feedback loop between OTUD5 and mTOR plays a role in regulating cell growth, cell proliferation, and autophagy.

## Discussion

In this study, we demonstrated a positive feedback loop between mTOR and OTUD5 to amplify mTORC1 and mTORC2 signaling. mTOR directly phosphorylates and activates OTUD5 (Fig. 5). In turn, the active OTUD5 stabilized  $\beta$ TrCP1, leading to the DEPTOR destruction and the mTOR activation (Figs. 1–3). This signaling can make a typical bistable switch induced by a positive feedback loop (Fig. 8). When it is “on” state, mTOR and OTUD5 are activated, leading to the induction of cell growth, proliferation, and the inhibition of autophagy. When it is “off” state, however, OTUD5 decreased, mTOR is inactivated, and the opposite events will occur. Therefore, the OTUD5-mTOR loop might switch on and off depending on the upstream signals such as growth factors and nutrients.

$\beta$ TrCP regulates a variety of pathways such as NF $\kappa$ B (nuclear factor  $\kappa$ B) [29], Hedgehog [30], and Wnt [23] as well as the mTOR signaling pathway [18–20] by targeting diverse substrates. Given that active mTOR increases the  $\beta$ TrCP1 protein level through OTUD5, the activity of the mTOR-OTUD5 pathway can also affect other signaling pathways to which  $\beta$ TrCP1 is involved. In this study, we showed that OTUD5 depletion enhanced the LEF-Luc activity and the *Armadillo* expression (Supplementary Fig. S5). These results suggested another layer of the crosstalk mechanism between mTOR and Wnt signaling in development and disease.

$\beta$ TrCP1 has been found to activate mTOR and inhibits autophagy by degrading DEPTOR [19, 31]. To determine whether the observed phenotypes by OTUD5 knockdown

were caused by degradation of  $\beta$ TrCP1, we tried to re-express  $\beta$ TrCP1 in OTUD5 depleted cells (Supplementary Fig. S9f). However, unfortunately, exogenous  $\beta$ TrCP1 did not accumulate in OTUD5 depleted cells, suggesting that OTUD5 is required for  $\beta$ TrCP1 protein stabilization.

OTUD5 has been found to control cell survival and cell proliferation by deubiquitination of p53 [32] and Ku80 [33] and interaction with FACT complex [34]. p53, one of the substrates of OTUD5, inhibits mTORC1 signaling by increasing TSC activity in DNA damage responses [35]. Nevertheless, the reason that OTUD5 depletion suppresses mTORC1/2 signaling to suppress cell proliferation is probably because OTUD5 accumulates DEPTOR downstream of TSC. UBR5 is, also a representative substrate of OTUD5 that is involved in cell survival and DNA damage response [36]. Because the UBR5 stability is controlled by OTUD5 [9], there is a possibility that the OTUD5 depletion phenotype is caused by the downregulated UBR5. However, we confirmed that UBR5 is not involved in the mTOR-OTUD5- $\beta$ TrCP1-DEPTOR pathway (Supplementary Fig. S9g, h).

Actually, a few studies have shown the functions of *Duba* in *Drosophila*. It was demonstrated that *Duba* is required for phagocytosis of *C. albicans* and male spermatogenesis [37, 38]. In terms of body and wing development, the whole body knockdown of *Duba* did not exhibit a significant phenotype [39]. Therefore, *Drosophila Duba per se* does not seem to affect the cell size.

The phosphorylation on Ser177 of OTUD5 by CK2 is essential for its DUB activity [24]. Ser177 phosphorylation facilitates the interaction with the ubiquitin substrate, which was essential for folding the N-terminal region of OTUD5 [24]. In this study, we showed that mTOR directly phosphorylated Ser323, Ser332, and Ser503 sites in OTUD5 and these phosphorylations affected not only its catalytic activity but also its stability. Of these three sites, Ser323 and Ser332 located near the catalytic triad (Cys224, His329, Asn331), might induce the structural changes of the catalytic triad through negative charge of the phosphates and affect the catalytic activity. Further detailed mechanistic studies are necessary to determine how the phosphorylations of OTUD5 by mTOR modulates its stability and DUB activity of OTUD5.

DEPTOR is an mTOR-interacting partner that suppresses the kinase activities of both mTORC1 and mTORC2 [17]. However, depending on the cellular context, DEPTOR has been shown to act as an activator of mTORC2 signaling [17, 40]. This phenomenon has been explained by the negative feedback mechanism formed between the mTORC1 and the PI3K-Akt pathway [17, 40]. However, our data indicated that OTUD5 could regulate both mTORC1 and mTORC2 signaling without being affected by negative feedback loops. Provided that hyperactivation of the PI3K pathway is one of the common events in human cancers [41] and high expression of OTUD5 is a poor

prognostic marker in some cancers (Supplementary Fig. S9i, j) [42], OTUD5 might be a good target for anticancer therapy with PI3K pathway hyperactivation, and the development of small molecule inhibitors of OTUD5 should be further investigated.

In conclusion, we have clearly demonstrated OTUD5 as a novel component in the mTOR signaling pathway that boosts the signaling via a positive feedback loop. It is highly plausible that the mTOR–OTUD5– $\beta$ TrCP1 signaling circuit may exert its effect on a variety of important pathways. Therefore, the physiological functions and therapeutic potential of OTUD5 should be further investigated.

Supplementary information is available at Cell Death & Differentiation's website.

**Acknowledgements** We would like to thank Dr. J. Chung (Seoul National University, Seoul) for a fly strain and Ms. H. Yoon (KRIBB, Daejeon) for a technical assistance on FACS and confocal microscopy. We would also like to thank our lab members for helpful discussions. The authors would like to thank Enago ([www.enago.co.kr](http://www.enago.co.kr)) for the English language review. This work was supported by the grant (CAP-15-11-KRICT) from National Research Council of Science and Technology, Ministry of Science and ICT, and the grant from KRIBB initiative program.

## Compliance with ethical standards

**Conflict of interest** The authors declare that they have no conflict of interest.

**Publisher's note** Springer Nature remains neutral with regard to jurisdictional claims in published maps and institutional affiliations.

## References

- Saxton RA, Sabatini DM. mTOR signaling in growth, metabolism, and disease. *Cell*. 2017;168:960–76.
- Liu P, Gan W, Chin YR, Ogura K, Guo J, Zhang J, et al. PtdIns(3,4,5)P<sub>3</sub>-dependent activation of the mTORC2 kinase complex. *Cancer Discov*. 2015;5:1194–209.
- Yang G, Murashige DS, Humphrey SJ, James DE. A positive feedback loop between Akt and mTORC2 via SIN1 phosphorylation. *Cell Rep*. 2015;12:937–43.
- Jiang Y, Su S, Zhang Y, Qian J, Liu P. Control of mTOR signaling by ubiquitin. *Oncogene*. 2019;38:3989–4001.
- Zhao L, Wang X, Yu Y, Deng L, Chen L, Peng X, et al. OTUB1 protein suppresses mTOR complex 1 (mTORC1) activity by deubiquitinating the mTORC1 inhibitor DEPTOR. *J Biol Chem*. 2018;293:4883–92.
- Wang B, Jie Z, Joo D, Ordureau A, Liu P, Gan W, et al. TRAF2 and OTUD7B govern a ubiquitin-dependent switch that regulates mTORC2 signalling. *Nature*. 2017;545:365–9.
- Hussain S, Feldman AL, Das C, Ziesmer SC, Ansell SM, Galaray PJ. Ubiquitin hydrolase UCH-L1 destabilizes mTOR complex 1 by antagonizing DDB1-CUL4-mediated ubiquitination of raptor. *Mol Cell Biol*. 2013;33:1188–97.
- Kayagaki N, Phung Q, Chan S, Chaudhari R, Quan C, O'Rourke KM, et al. DUBA: a deubiquitinase that regulates type I interferon production. *Science*. 2007;318:1628–32.
- Rutz S, Kayagaki N, Phung QT, Eidenschenk C, Noubade R, Wang X, et al. Deubiquitinase DUBA is a post-translational brake on interleukin-17 production in T cells. *Nature*. 2015;518:417–21.
- Cho JH, Kim SA, Seo YS, Park SG, Park BC, Kim JH, et al. The p90 ribosomal S6 kinase-UBR5 pathway controls Toll-like receptor signaling via miRNA-induced translational inhibition of tumor necrosis factor receptor-associated factor 3. *J Biol Chem*. 2017;292:11804–14.
- Sarbasov DD, Ali SM, Kim DH, Guertin DA, Latek RR, Erdjument-Bromage H, et al. Rictor, a novel binding partner of mTOR, defines a rapamycin-insensitive and raptor-independent pathway that regulates the cytoskeleton. *Curr Biol*. 2004;14:1296–302.
- Frank SB, Schulz VV, Miranti CK. A streamlined method for the design and cloning of shRNAs into an optimized Dox-inducible lentiviral vector. *BMC Biotechnol*. 2017;17:24.
- Heckl D, Kowalczyk MS, Yudovich D, Belizaire R, Puram RV, McConkey ME, et al. Generation of mouse models of myeloid malignancy with combinatorial genetic lesions using CRISPR-Cas9 genome editing. *Nat Biotechnol*. 2014;32:941–6.
- Dobin A, Davis CA, Schlesinger F, Drenkow J, Zaleski C, Jha S, et al. STAR: ultrafast universal RNA-seq aligner. *Bioinformatics*. 2013;29:15–21.
- McCarthy DJ, Chen Y, Smyth GK. Differential expression analysis of multifactor RNA-Seq experiments with respect to biological variation. *Nucleic Acids Res*. 2012;40:4288–97.
- Mootha VK, Lindgren CM, Eriksson KF, Subramanian A, Sihag S, Lehar J, et al. PGC-1 $\alpha$ -responsive genes involved in oxidative phosphorylation are coordinately downregulated in human diabetes. *Nat Genet*. 2003;34:267–73.
- Peterson TR, Laplante M, Thoreen CC, Sancak Y, Kang SA, Kuehl WM, et al. DEPTOR is an mTOR inhibitor frequently overexpressed in multiple myeloma cells and required for their survival. *Cell*. 2009;137:873–86.
- Duan S, Skaar JR, Kuchay S, Toschi A, Kanarek N, Ben-Neriah Y, et al. mTOR generates an auto-amplification loop by triggering the  $\beta$ TrCP- and CK1 $\alpha$ -dependent degradation of DEPTOR. *Mol Cell*. 2011;44:317–24.
- Gao D, Inuzuka H, Tan MK, Fukushima H, Locasale JW, Liu P, et al. mTOR drives its own activation via SCF( $\beta$ TrCP)-dependent degradation of the mTOR inhibitor DEPTOR. *Mol Cell*. 2011;44:290–303.
- Zhao Y, Xiong X, Sun Y. DEPTOR, an mTOR inhibitor, is a physiological substrate of SCF( $\beta$ TrCP) E3 ubiquitin ligase and regulates survival and autophagy. *Mol Cell*. 2011;44:304–16.
- Frescas D, Pagano M. Deregulated proteolysis by the F-box proteins SKP2 and  $\beta$ -TrCP: tipping the scales of cancer. *Nat Rev Cancer*. 2008;8:438–49.
- Jiang J, Struhl G. Regulation of the Hedgehog and Wingless signalling pathways by the F-box/WD40-repeat protein Slimb. *Nature*. 1998;391:493–6.
- Liu C, Kato Y, Zhang Z, Do VM, Yankner BA, He X.  $\beta$ -Trop couples  $\beta$ -catenin phosphorylation-degradation and regulates Xenopus axis formation. *Proc Natl Acad Sci USA*. 1999;96:6273–8.
- Huang OW, Ma X, Yin J, Flinders J, Maurer T, Kayagaki N, et al. Phosphorylation-dependent activity of the deubiquitinase DUBA. *Nat Struct Mol Biol*. 2012;19:171–5.
- Fingar DC, Salama S, Tsou C, Harlow E, Blenis J. Mammalian cell size is controlled by mTOR and its downstream targets S6K1 and 4EBP1/eIF4E. *Genes Dev*. 2002;16:1472–87.
- Stocker H, Radimerski T, Schindelhof B, Wittwer F, Belawat P, Daram P, et al. Rheb is an essential regulator of S6K in controlling cell growth in Drosophila. *Nat Cell Biol*. 2003;5:559–65.

27. Kimura S, Noda T, Yoshimori T. Dissection of the autophagosome maturation process by a novel reporter protein, tandem fluorescent-tagged LC3. *Autophagy*. 2007;3:452–60.
28. Meric-Bernstam F, Akcakanat A, Chen H, Do KA, Sangai T, Adkins F, et al. PIK3CA/PTEN mutations and Akt activation as markers of sensitivity to allosteric mTOR inhibitors. *Clin Cancer Res*. 2012;18:1777–89.
29. Yaron A, Hatzubai A, Davis M, Lavon I, Amit S, Manning AM, et al. Identification of the receptor component of the I $\kappa$ B $\alpha$ -ubiquitin ligase. *Nature*. 1998;396:590–4.
30. Bhatia N, Thiyagarajan S, Elcheva I, Saleem M, Dlugosz A, Mukhtar H, et al. Gli2 is targeted for ubiquitination and degradation by beta-TrCP ubiquitin ligase. *J Biol Chem*. 2006;281:19320–6.
31. Xiong X, Liu X, Li H, He H, Sun Y, Zhao Y. Ribosomal protein S27-like regulates autophagy via the beta-TrCP-DEPTOR-mTORC1 axis. *Cell Death Dis*. 2018;9:1131.
32. Luo J, Lu Z, Lu X, Chen L, Cao J, Zhang S, et al. OTUD5 regulates p53 stability by deubiquitinating p53. *PLoS One*. 2013;8:e77682.
33. Li F, Sun Q, Liu K, Han H, Lin N, Cheng Z, et al. The deubiquitinase OTUD5 regulates Ku80 stability and non-homologous end joining. *Cell Mol Life Sci*. 2019;76:3861–73.
34. de Vivo A, Sanchez A, Yegres J, Kim J, Emly S, Kee Y. The OTUD5-UBR5 complex regulates FACT-mediated transcription at damaged chromatin. *Nucleic Acids Res*. 2019;47:729–46.
35. Feng Z, Hu W, de Stanchina E, Teresky AK, Jin S, Lowe S, et al. The regulation of AMPK beta1, TSC2, and PTEN expression by p53: stress, cell and tissue specificity, and the role of these gene products in modulating the IGF-1-AKT-mTOR pathways. *Cancer Res*. 2007;67:3043–53.
36. Shearer RF, Iconomou M, Watts CK, Saunders DN. Functional roles of the E3 ubiquitin ligase UBR5 in cancer. *Mol Cancer Res*. 2015;13:1523–32.
37. Stroschein-Stevenson SL, Foley E, O'Farrell PH, Johnson AD. Identification of *Drosophila* gene products required for phagocytosis of *Candida albicans*. *PLoS Biol*. 2006;4:e4.
38. Koerver L, Melzer J, Roca EA, Teichert D, Glatter T, Arama E, et al. The de-ubiquitylating enzyme DUBA is essential for spermatogenesis in *Drosophila*. *Cell Death Differ*. 2016;23:2019–30.
39. Tsou WL, Sheedlo MJ, Morrow ME, Blount JR, McGregor KM, Das C, et al. Systematic analysis of the physiological importance of deubiquitinating enzymes. *PLoS One*. 2012;7:e43112.
40. Caron A, Briscoe DM, Richard D, Laplante M. DEPTOR at the nexus of cancer, metabolism, and immunity. *Physiol Rev*. 2018;98:1765–803.
41. Thorpe LM, Yuzugullu H, Zhao JJ. PI3K in cancer: divergent roles of isoforms, modes of activation and therapeutic targeting. *Nat Rev Cancer*. 2015;15:7–24.
42. Mizuno H, Kitada K, Nakai K, Sarai A. PrognoScan: a new database for meta-analysis of the prognostic value of genes. *BMC Med Genom*. 2009;2:18.